FABRICATION OF SHAPE MEMORY ALLOYS USING THE PLASMA SKULL PUSH-PULL PROCESS

Antonio Aristófanes da Cruz Gomes, antonioaristofanes@yahoo.com.br
Jobson Alberto Silva, jobson.alberto@gmail.com
Ângelo José Tavares Cavalcanti, angelojstc@hotmail.com
Rômulo Pierre Batista dos Reis, soromulo@hotmail.com
Carlos José de Araújo, carlos@dem.ufcg.edu.br
Multidisciplinary Laboratory on Active Materials and Structures
Department of Mechanical Engineering
Universidade Federal de Campina Grande
Caixa Postal: 10069, Cep: 58109-970
Campina Grande – PB, Brazil

Cezar Henrique Gonzalez, gonzalez@ufpe.br
Department of Mechanical Engineering
Universidade Federal de Pernambuco
Av. Acadêmico Hélio Ramos, s/n - Cidade Universitária
Cep: 50740-530, Recife – PE, Brazil

Abstract. *In this work, fabrication of shape memory alloys (SMA) employing the plasma skull push-pull (PSPP) process was studied. In this process, very small quantities of metallic elements can be quickly melted on a copper crucible by a rotative plasma torch and injected in a metallic mold. In order to validate the utilization of the PSPP process to produce SMA, several Ni-Ti based and Cu-Al based binary, ternary and quaternary alloys were tested. It was verified that five melts and re-melts of the SMA before injection are enough to obtain an homogeneous product. The obtained SMA were characterized by optical microscopy and microhardness measurements. The thermoelastic martensitic transformation at the origin of the shape memory effect (SME) was studied by electrical resistance as a function of temperature and differencial scanning calorimetry (DSC). All studied SMA have presented the thermoelastic transformation demonstrating the viability of the PSPP process to fabricate a great variety of SMA.*

Keywords*: Shape memory alloys, Plasma skull, Ni-Ti alloys, Metal injection molding.*

1. INTRODUCTION

Shape memory alloys (SMA) are functional metallic materials that can respond to a temperature change producing an important macroscopic deformation. These special metallic alloys are for the most part of two families: copper based alloys (Cu-Zn-Al, Cu-Al-Ni, Cu-Al-Mn,....) and Ni-Ti based alloys (Ni-Ti, Ni-Ti-Cu, Ni-Ti-Nb,....). The industrial and laboratory scale production of these materials is carried out using different processes, as Air Induction Melting (AIM), Vacuum Induction Melting (VIM) (Zhang *et al*, 2005; Rigo *et al*, 2005), Vacuum consumable and non-consumable Arc Melting (VAM) (Wu, 2001), Electron Beam Melting (EBM) (Otubo *et al*, 2004), Powder Metallurgy (PM) (Bram *et al*, 2002; Shaw *et al*, 2002), Rapid Solidification (mainly *Melt-Spinning*) (Lin & Wu, 2006; Kim *et al*, 2006) and Mechanical Alloying (MA) (Li *et al*, 2006). However, few information exist about the application of processes that use the plasma melting technology to produce SMA. The influence of some melting techniques to obtain Ni-Ti SMA was discussed by Russel (2001).

The Argon non-consumable electrode Arc Melting (AAM) is preferred in laboratories because it is applicable to many kinds of alloys (Otsuka & Wayman, 1998). In this method, raw metallic elements are installed on a copper crucible and irradiated by the argon arc from a tungsten electrode. The obtained button is turned over and remelted repeatedly to improve the homogeneity of the composition. The Plasma Arc Melting (PAM) method uses a low velocity electron beam discharged from a plasma cathode. According to Otsuka & Wayman (1998), compared to the hard irradiation of from a high voltage of EBM or AAM, electron irradiation from the plasma cathode is milder. It results in low loss of the alloy elements. The basic advantages of plasma melting furnaces are (a) fast melting rates, (b) negligible or no carbon contamination, (c) vacuum quality melts, (d) stable power – less voltage fluctuation, (e) lower cost of furnace installation compared to VIM and VAM, (f) no loss of high vapor pressure metals in plasma furnaces operated with inert gases, and others (Bhat, 1972). Additionally, in the plasma skull method, melting is accomplished on a fine layer of the own metal reducing the possibility of contamination by the crucible.

In this work, fabrication of binary, ternary and quaternary SMA by plasma melting is studied. The employed process was melting and casting by Plasma Skull Push Pull (PSSP) where the alloy is melted on a thin layer of even her in a copper crucible and later injected into a cylindrical aluminum mold. Then, this technique is a combination of PAM with Metal Injection Molding (MIM). Ni-Ti and Cu-Al based SMA produced by this process were characterized by optical microscopy, microhardness and electrical resistance as a function of temperature.

2. EXPERIMENTAL PROCEDURE

The raw materials used to produce the Cu-Al based SMA were commercial pure metals (>99,9%). In the case of Ni-Ti SMA, it was employed the ASTM F67-00 (grade 2) biomedical titanium. In Table 1 the nominal chemical composition and main characteristics of each investigated SMA is given. A small amount (20 – 30 g) of each SMA was produced by the Plasma Skull Push Pull (PSPP) process using the Discovery All Metals equipment (EDG Equipamentos e Controles, Brazil).

Table 1. Nominal chemical composition of the studied SMA.

SMA code	Nominal composition (wt %)	Main expected characteristics
NiTi-1	55Ni-45Ti	Classical Ni-Ti SMA presenting R-phase (Otsuka & Ren, 2005)
NiTi-2	55,16Ni-44,84Ti	Classical Ni-Ti SMA presenting R-phase (Otsuka & Ren, 2005)
NiTi-3	49,4Ni-44,7Ti-5,9Cu	Remove R-phase and reduce thermal hyteresis (Nam *et al*, 1990)
NiTi-4	48Ni-38Ti-14Nb	High hysteresis Ni-Ti SMA (Zhao *et al*, 2006)
CuAl-1	82,5Cu-13,5Al-4,0Ni	Cu-Al-Ni SMA with TT<100^{o}C (Otsuka & Wayman, 1998)
CuAl-2	82,5Cu-13,2Al-4,0Ni-0,3Mn	Improve ductility of Cu-Al-Ni SMA (Otsuka & Wayman, 1998)
CuAl-3	82,5Cu-13,2Al-4,0Ni-0,3Nb	Increase TT of Cu-Al-Ni SMA (Lelatko & Morawiec, 2003)

*TT – Transformation Temperatures

Figure 1 shows a typical PSPP sequence for a Ni-Ti SMA. Ni and Ti are initially pilled up on a copper crucible (Fig. 1a) and submitted to a protective argon atmosphere. Melting of the raw elements is rapidly performed with a rotative plasma torch created by a tungsten electrode (Fig. 1b), originating a small bottom (Fig. 1c). In order to assure a good homogeneity of the SMA, it was verified that five melt and re-melts must be realized. The final product is obtained when the re-melted bottom (Fig. 1d) is injected in a metallic mold (Fig. 1e) originating a tablet (Fig. 1f) or other final form. Cu-Al based SMA are produced following the same sequence of Fig. 1.

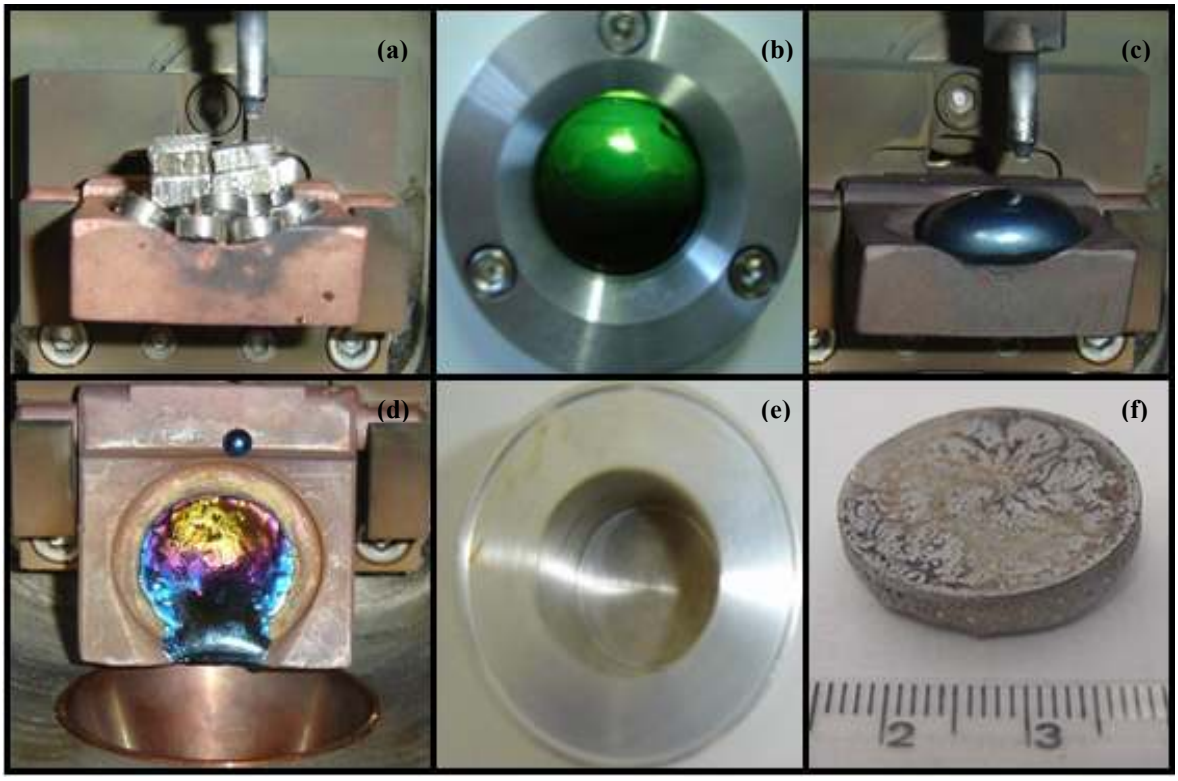

Figure 1. Melting and injection molding sequence of the PSPP process. (a) Pilled up raw materials. (b) Rotative plasma torch. (c) SMA bottom. (d) SMA layer on the crucible after mold injection. (e) Metallic mold. (f) SMA tablet.

The PSPP process described in Fig. 1 is extremely fast. Figure 2 show the temperature evolution of the copper crucible (Fig. 1c) during the melting of a stainless steel sample of about 22 g. For this measurement a micro-

thermocouple (K type, 80 μm in diameter) was installed in the crucible, at about 4 mm from the melt. It can be noted from Fig. 2 that melting is finalized after about 15 s.

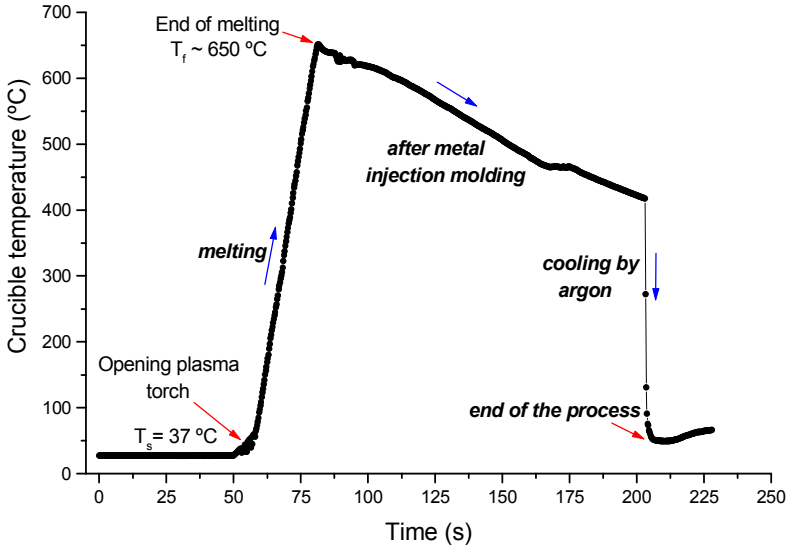

Figure 2. Time of melting and molding of a stainless steel sample by the PSPP process.

Specimens cutted off from the SMA tablets (Fig. 1f) were prepared for metallographic observations using optical microscopy (Olimpus, BX51M) and microhardness measurements (Future-Tech, FM-700). All samples were betatized at 850 °C for 900 s and water quenched. The apparition of the thermoelastic martensitic transformation (TMT) was verified by electrical resistance as a function of temperature using an apparatus specially designed for this task (Reis *et al*, 2006). For some SMA with low transformation temperatures (TT < 10 °C), thermal analysis by DSC (Mettler, TA-3000) was employed to detect the TMT.

3. RESULTS AND DISCUSSIONS

As can be observed in Fig. 1(d), the final product of the PSPP process is a SMA tablet. However, Fig. 3 shows that adaptation of some steel components, as tube and pin, in the metallic mold (Fig. 3a) allow to fabricate others semi-finished products like small rods and tubes (Figs. 3b and 3c). Though there is a change in size, good dimensional accuracy is achieved by the PSPP process.

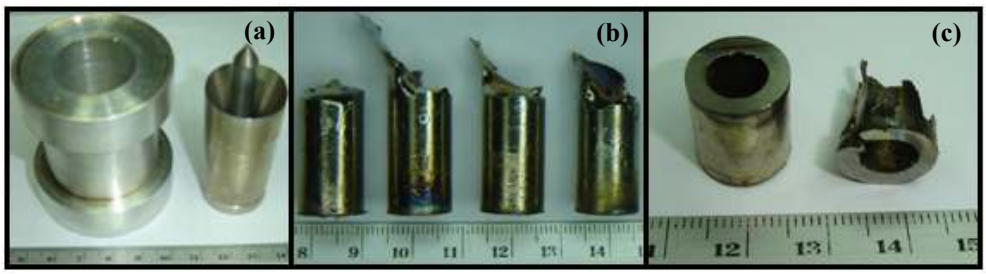

Figure 3. Some SMA parts obtained by PSPP process. (a) Adaptation of the metallic mold. (b) Ni-Ti mini rods. (c) Ni-Ti mini tubes.

3.1. Ni-Ti based SMA

Figure 4 shows the typical microstructure of the Ni-Ti based SMA summarized in Tab. 1 (NiTi-1 and NiTi-3). It is well known that Ni-Ti SMA presents very fine grains difficult to visualize by optical microscopy (Otsuka & Wayman, 1998). Then, as expected, it can be also observed from Fig.4 that there is no trace of martensite plates. The microstructure of Fig. 4(a) is similar to the one observed by Chang *et al* (2005).

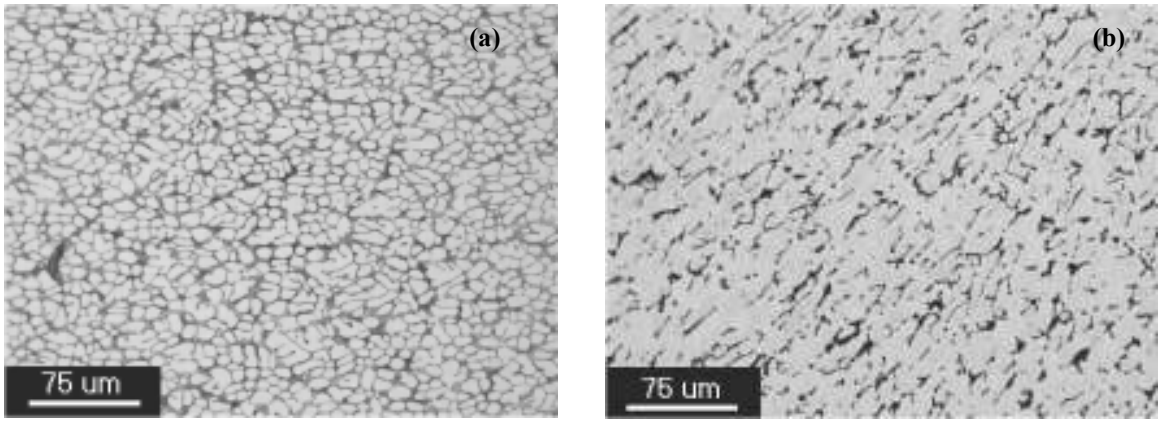

Figure 4. Microstructures of (a) NiTi-1 and (b) NiTi-3 SMA.

Comparing Figs. 4(a) and 4(b), it can be verified that Cu addition in substitution to Ni changes the morphology of the binary Ni-Ti SMA. On the other hand, it was observed that morphology of the 48Ni-38Ti-14Nb (NiTi-4), and others Ni-Ti binary SMA (NiTi-2), are very similar to the one of 55Ni-45Ti (NiTi-1, Fig. 4a). These microstructures present the hardness values summarized in Tab. 2.

Table 2. Vickers microhardness (HV) values for the Ni-Ti based SMA.

SMA code	Microhardness - Water quenched (HV)
NiTi-1	229,3 ± 12,8
NiTi-2	----
NiTi-3	208,4 ± 16,0
NiTi-4	260,5 ± 27,8

Figure 5 show the transformation behaviors of the Ni-Ti binary SMA (NiTi-1 and NiTi-2) verified by electrical resistance as a function of temperature (ER – T).

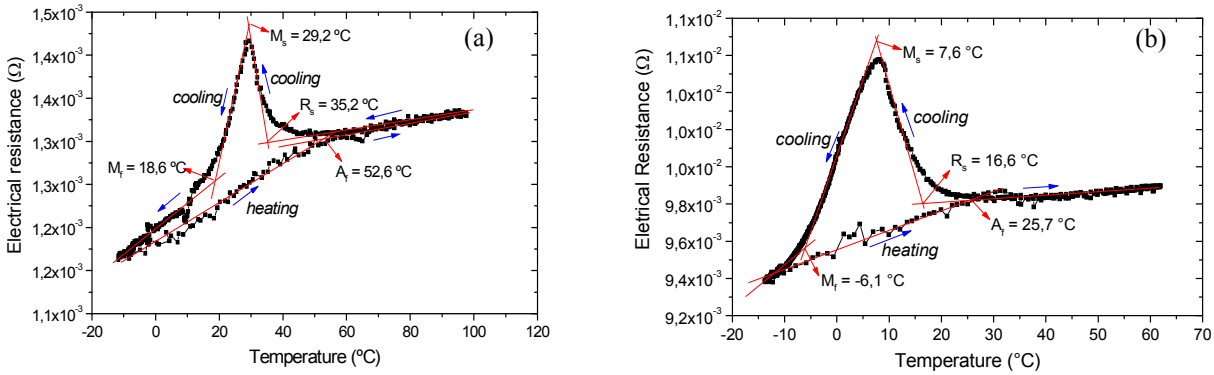

Figure 5. ER – T behavior of (a) NiTi-1 and (b) NiTi-2.

For these binary SMA it was observed that transformation occurs in two steps, from cubic austenite (B2) to an intermediary rhombohedric phase (R) and then to the monoclinic martensite (B19'). The appearance of the R-phase originates an important peak in the ER – T behavior during cooling. As noticed in the literature (Otsuka & Wayman, 1998; Otsuka & Ren, 2005), reversion of the B19'-R- B2 transformation during heating is not visible. Figure 5 also demonstrate that increasing Ni content in about 0,15 %wt, transformation temperatures are reduced of approximately 20 °C. According to Wu (2001), for alloys having greater than 55,0 %wt Ni, a one weight percent deviation in Ni (or Ti) concentration will result in approximately a 100°C shift in transformation temperatures. This extreme sensitivity puts a strict requirement on any melting practice to tightly control the Ni and Ti ratio in order to meet the required tolerance in transformation temperatures. The results presented in Fig. 5 confirm that the PSPP process can provide these requirements.

Some compositions of ternary Ni-Ti based SMA, like Ni-Ti-Cu and Ni-Ti-Nb, present a single transformation, from B2 to B19'. Figure 6 shows the ER – T and DSC results for the ternary Ni-Ti-Cu and Ni-Ti-Nb SMA (NiTi-3 and NiTi-4) produced by the PSPP process.

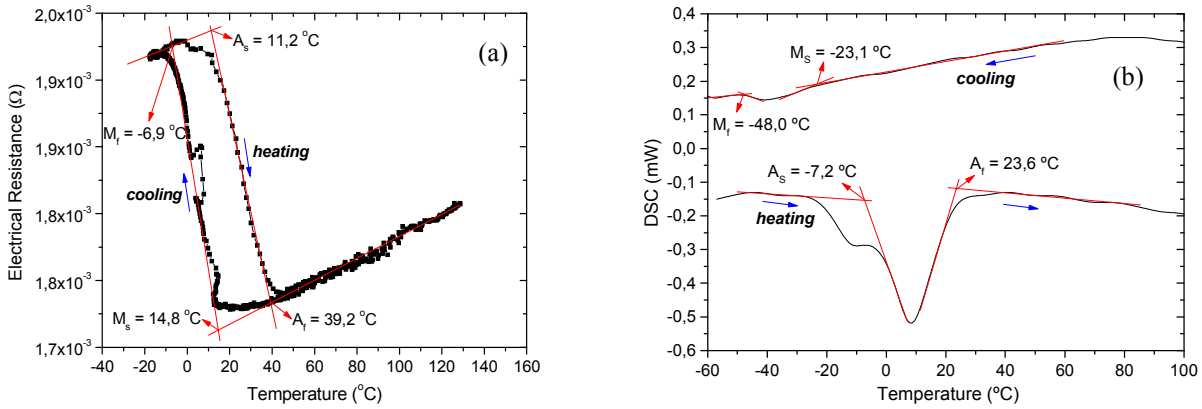

Figure 6. Transformation behavior of the Ni-Ti-Cu and Ni-Ti-Nb SMA. (a) ER – T characteristic of NiTi-3 and (b) DSC of NiTi-4.

Addition of a small amount of Cu (< 7,5 %at) in substitution to Ni eliminate the R-phase originating a classical ER – T loop corresponding to a single B2 to B19' transformation (Nam *et al*, 1990), as confirmed in Fig. 6(a). In general, ternary Ni-Ti-Nb SMA also present a single B2 to B19' transformation characterized by a large thermal hysteresis (Zhao *et al*, 2006). The DSC curve of Fig. 6(b) show that thermal hysteresis of the Ni-Ti-Nb produced by PSPP was of the order of 50 °C. Table 3 show all transformation temperatures obtained directly from Figs. 5 and 6.

Table 3. Transformation temperatures for the studied Ni-Ti based SMA.

	Transformation Temperatures (°C)				
SMA code	M_f	M_s	R_s	A_s	A_f
NiTi-1	18,6	29,2	35,2	-	52,6
NiTi-2	-6,1	7,6	16,6	-	25,7
NiTi-3	-6,9	14,8	-	11,2	39,2
NiTi-4	-48,0	-23,1	-	-7,2	23,6

3.2. Cu-Al based SMA

Figure 7 show all martensitic microstructures and corresponding ER – T curves for the Cu-Al based SMA defined in Tab.1. Contrarily to the Ni-Ti based SMA, it is possible to identify large grains with martensite plates (Figs. 7a, 7c and 7e) commonly observed in Cu-Al based SMA (Lin *et al*, 2000) and single step transformations (Figs. 7b, 7d and 7f) characterized by a narrow thermal hysteresis (10 to 15 °C). Figure 7(b) show that the M_s temperature for the Cu-13,5Al-4,0Ni (CuAl-1) is of the order of 83 °C. According to Recarte *et al* (1999), M_s temperatures between 30 °C and 120 °C are measured in Cu-Al-Ni SMA with a Ni content of 4 %wt and Al in the range 13,0-13,8 %wt. As demonstrated in Fig. 7(d), addition of 0,3 %wt Mn in substitution to Al in the ternary Cu-Al-Ni SMA maintains unaffected the transformation. However, Fig. 7(f) show that the same substitution using 0,3 %wt Nb increase the transformation temperatures of about 50 °C. Ternary Cu-Al-Nb are SMA characterized by transformation temperatures higher than 200 °C (Lelatko & Morawiec, 2003).

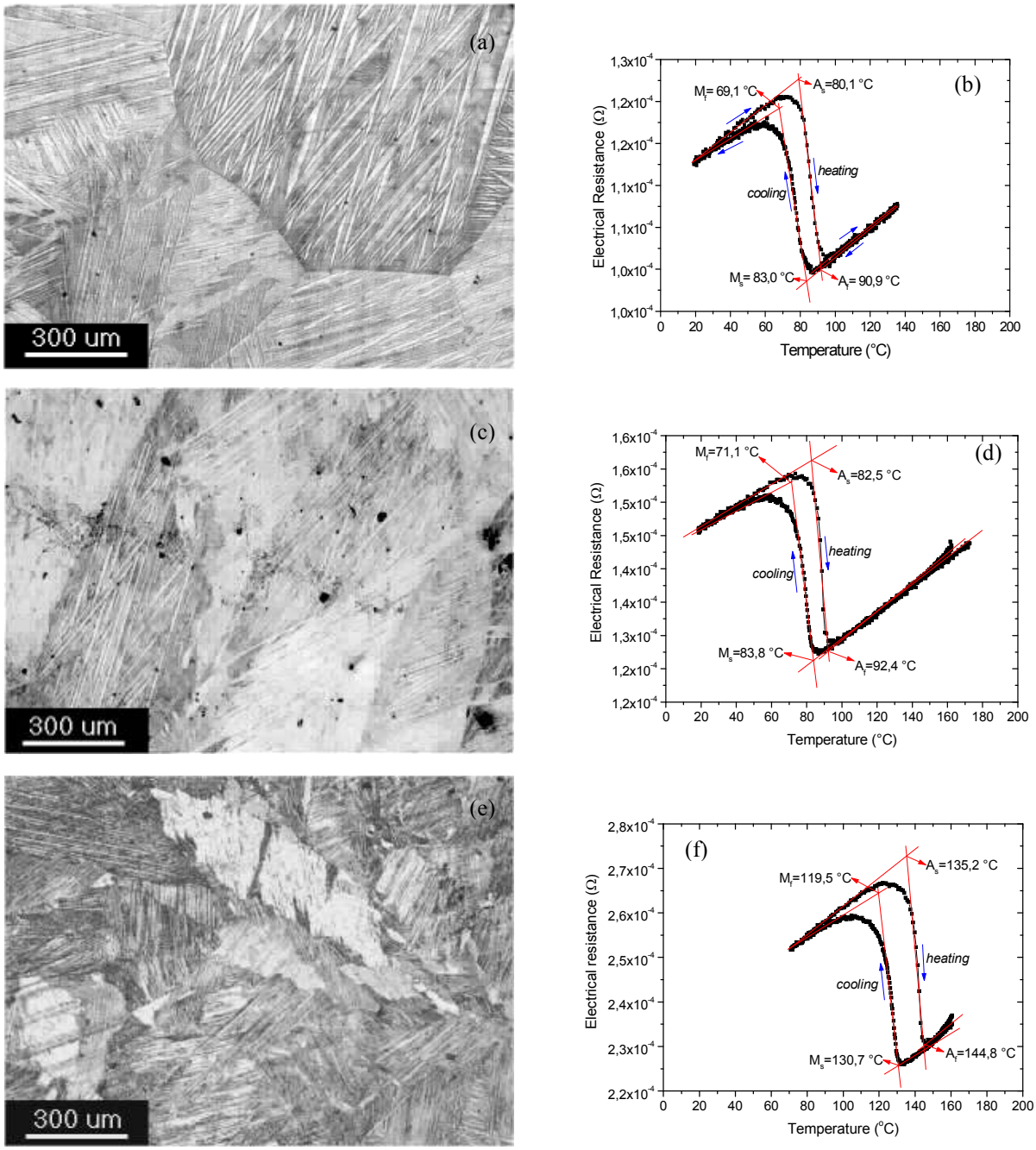

Figure 7. Microstructure and transformation behavior of the Cu-Al based SMA. (a,b) CuAl-1. (c,d) CuAl-2. (e,f) CuAl-3.

It is well known that ductility of Cu-Al-Ni SMA decreases significantly with a small increase of Al content. However, substitution of Al by Mn improves the ductility substantially without taking to important modifications in the transformation temperatures (Otsuka & Wayman, 1998). The table 4 summarizes the hardness of each studied Cu-Al based SMA. This table confirm that martensitic microstructure of the Cu-Al-Ni-Mn (CuAl-2) present the smallest hardness. It is also verified that the microstructure of the as-produced Cu-Al SMA is partially martensitic and present hardness values higher than the ones of the fully martensitic water quenched microstructure.

Table 4. Vickers microhardness (HV) values for the Cu-Al based SMA.

SMA code	Microhardness - As-fabricated (HV)	Microhardness - Water quenched (HV)
CuAl-1	308,1 ± 20,4	236,1 ± 12,3
CuAl-2	335,2 ± 17,5	209,7 ± 19,5
CuAl-3	304,7 ± 12,4	241,9 ± 13,2

4. CONCLUSIONS

It was demonstrated that several kinds of shape memory alloys (SMA) can be manufactured by the plasma skull push pull method (PSPP). Working on the design of molds for the PSPP process make possible the fabrication of different small semi-finished products, like tablets, tubes, rod bars, prismatic bars and others. The occurrence of the thermoelastic martensitic transformation at the origin of the shape memory phenomena for all studied SMA was proven by electrical resistance as a function of the temperature. The study of binary Ni-Ti SMA with a difference of 0,15 %wt in the Ni content as well as modification of this SMA by adding Cu and Nb, have confirmed the capacity of PSPP method to control chemical composition and produce high quality alloys with expected transformation temperatures. The PSPP process was also effective for the production of Cu-Al based SMA demonstrating clearly the influence of small contents of Mn and Nb in substitution of Al in ternary Cu-Al-Ni SMA.

5. ACKNOWLEDGEMENTS

The authors thank the Conselho Nacional de Desenvolvimento Científico e Tecnológico (CNPq), Brazilian office for sponsoring the research (CT-Energ grant 550325/2005-0 and CT-Petro grant 504365/2004-5) during the course of these investigations.

6. REFERENCES

Bhat, G. K., 1972. "New developments in plasma arc melting", Journal of Vacuum Science and Technology, Vol. 9, N° 6, pp. 1344 – 1350.

Bram, M., Ahmad-Khanlou, A., Heckmann, A., Fuchs, B., Buchkremer, H. P., Stover, D., 2002. "Powder metallurgical fabrication processes for NiTi shape memory alloy parts", Materials Science and Engineering A, Vol. 337, pp. 254 - 263.

Chang, S. H., Wu, S. K., Chang, G. H., 2005. "Grain size effect on multiple-stage transformations of a cold-rolled and annealed equiatomic TiNi alloy", Scripta Materialia, Vol.52, pp.1341–1346.

Kim, Y., Yun, Y., Nam, T., 2006. "The effect of the melt spinning processing parameters on the solidification structures in Ti–30 at.% Ni–20 at.% Cu shape memory alloys", Materials Science and Engineering A, Vol. 438–440, pp. 545–548.

Lelatko, J. and Morawiec, H., 2003. "The effect of Ni, Co and Cr on the primary particle structure in Cu–Al–Nb–X shape memory alloys", Materials Chemistry and Physics, Vol. 81, pp. 472–475.

Li, Z., Pan, Z.Y., Tang, N., Jiang, Y.B., Liu, N., Fang, M., Zheng, F., 2006. "Cu–Al–Ni–Mn shape memory alloy processed by mechanical alloying and powder metallurgy", Materials Science and Engineering A, Vol. 417, pp. 225–229.

Lin, K. N., Wu, S. K., 2006. "Martensitic transformation of grain-size mixed $Ti_{51}Ni_{49}$ melt-spun ribbons", Journal of Alloys and Compounds, Vol. 424, pp. 171–175.

Lin, Z.C., Yu, W., Zee, R.H., Chin, B.A., 2000. "CuAlPd alloys for sensor and actuator applications", Intermetallics, Vol. 8, pp. 605 – 611.

Nam, T. H., Saburi, T., Shimizu, K., 1990. "Cu-content dependence of shape memory characteristics in Ti-Ni-Cu alloys", Materials Transactions JIM, Vol. 31, n° 11, pp. 959 – 967.

Otsuka, K., Wayman, C.M., 1998. "Shape Memory Materials", Cambridge University Press, Cambridge, UK, 284p.

Otsuka, K., Ren, X., 2005. "Physical metallurgy of Ti –Ni-based shape memory alloys", Progress in Materials Science, Vol. 50, pp. 511-678.

Otubo, J., Rigo, O. D., Moura Neto, C., Kaufman, M. J., Mei, P. R., 2004. "Low carbon content NiTi shape memory alloy produced by electron beam melting", Materials Research, Vol. 7, No. 2, pp. 263-267.

Recarte, V., Perez-Saez, R.B., Bocanegra, E.H., Nó, M.L., San Juan, J., 1999. "Dependence of the martensitic transformation characteristics on concentration in Cu–Al–Ni shape memory alloys", Materials Science Engineering A, Vol. 273-275, pp. 380-384.

Reis, R. P. B., de Araújo, C. J., Silva, L. A. R., Queiroga, S. L. M., 2006. "Desenvolvimento de um sistema de medição da variação de resistência elétrica em função da temperatura: aplicação a caracterização de ligas com memória de forma", Proceedings of Forth National Congress of Mechanical Engineering (CONEM 2006), Recife – PE, Brazil, pp. 1 – 10. *In portuguese.*

Rigo, O. D., Otubo, J., Moura Neto, C., Mei, P. R., 2005. "NiTi SMA production using ceramic filter during pouring the melt", Journal of Materials Processing Technology, Vol. 162–163, pp. 116–120.

Russel, S. M., 2001. "Nitinol melting and fabrication", Proceedings of the International Conference on Shape Memory and Superelastic Technologies, Eds. S.M. Russell and A.R. Pelton, (Pacific Grove, California: International Organization on SMST, 2001), pp. 1 – 10.

Shaw, J. A., Gremillet, A., Grummon, D. S., 2002. "The manufacture of NiTi foams", Proceedings of 2002 ASME International Mechanical Engineering Congress and Exposition, New Orleans, LA, USA, pp. 1 – 10.

Wu, M. H., 2001. "Fabrication of Nitinol Materials and Components", Proceedings of the International Conference on Shape Memory and Superelastic Technologies, Kunming, China, pp.285-292.

Zhao, X., Yan, X., Yang, Y., Xu, H., 2006. "Wide hysteresis NiTi(Nb) shape memory alloys with low Nb content (4.5 at.%)", Materials Science and Engineering A, Vol. 438–440, pp. 575–578.

Zhang, Z., Frenzel, J., Neuking, K., Eggeler, G., 2005. "On the reaction between NiTi melts and crucible graphite during vacuum induction melting of NiTi shape memory alloys", Acta Materialia, Vol. 53, pp. 3971–3985.